32

JAERI-RESEARCH-98-041

SEP 16 1998

Fermilab Library
0 1160 0067550 8

JAERI-Research
98-041

RF CONTROL AT TRANSIENT BEAMLOADING FOR HIGH-DUTY-FACTOR LINACS

August 1998

NAME | No. | M.S.

RETURN TO FERMILAB LIBRARY

Michael A. CHERNOGUBOVSKY and Masayoshi SUGIMOTO

日本原子力研究所
Japan Atomic Energy Research Institute

本レポートは，日本原子力研究所が不定期に公刊している研究報告書です。
入手の問合わせは，日本原子力研究所研究情報部研究情報課（〒319-1195　茨城県那珂郡東海村）あて，お申し越しください。なお，このほかに財団法人原子力弘済会資料センター（〒319-1195　茨城県那珂郡東海村日本原子力研究所内）で複写による実費頒布をおこなっております。

This report is issued irregularly.
Inquiries about availability of the reports should be addressed to Research Information Division, Department of Intellectual Resources, Japan Atomic Energy Research Institute, Tokai-mura, Naka-gun, Ibaraki-ken, 319-1195, Japan.

© Japan Atomic Energy Research Institute, 1998

編集兼発行　　日本原子力研究所

JAERI-Research 98-041

RF Control at Transient Beamloading for High-duty-factor Linacs

Michael A. CHERNOGUBOVSKY* and Masayoshi SUGIMOTO

Department of Materials Science
Tokai Research Establishment
Japan Atomic Energy Research Institute
Tokai-mura, Naka-gun, Ibaraki-ken

(Received July 9, 1998)

An effective RF control with the transient beamloading is the major issue in the operation of the high-duty-factor linacs to suppress the undesirable beam loss. The RF control method is considered to obtain the control principle and the state equation,under the analysis of electrodynamical properties of the excitation in the resonator of the linac due to the transient beamloading. The concept of the directional selective coupling is applied for the RF system to define the main characteristics and to optimize the RF control parameters.

Keywords: Accelerator, RF control, Beamloading, Transient, Resonator, Directional Selective Coupling

* Research Fellow

JAERI-Research 98-041

高デューティーのリニアックに過渡的ビーム負荷がかかる場合の高周波制御

日本原子力研究所東海研究所物質科学研究部
Michael A. CHERNOGUBOVSKY※・杉本　昌義

(1998年7月9日受理)

高いデューティーでリニアックを運転する場合に大きな問題となるのは、過渡的なビーム負荷の下で如何に効率よく高周波の制御を行い、ビームロスを少なくするかという点である。そのような場合の高周波制御方式を確立する為に、過渡的に負荷が変わるようなビームによる空洞の励振特性を解析することによって、制御の原理及び状態方程式を導いた。方向性選択結合の考えを高周波システムに適用することで、システムの主要な特性を決定し、高周波制御パラメータの最適化を図った。

東海研究所　〒319－1195　茨城県那珂郡東海村白方白根2－4
※　原研リサーチフェロー

Contents

1. Introduction 1
2. RFGeneral Characteristics 1
2.1 Setting of the Problem 1
2.2 Accelerator RF System 2
2.3 Control Principles 3
2.4 External Characteristics 6
2.5 Control Signal Properties 7
2.5.1 RF Signal Energy Relations 7
2.5.2 Modulation Laws 9
2.5.3 Tuning Characteristics 9
2.6 Resume 10
3. General for Optimization 10
4. RF Signal Determination 12
5. Accelerating Channel Characteristics 16
6. Conclusion 17
References 19
Appendix 1. Detailed Analysis of Resonator Electromagnetic Field at Arbitrary Excitations 21
A1.1 Electrodynamical Set Properties 21
A1.2 Excitation 22
A1.3 Wall Losses 23
Appendix 2. 26
Appendix 3. 26
Appendix 4. 27
Appendix 5. 28
Appendix 6. 29

目　　次

1. はじめに …… 1
2. 高周波の一般的特性 …… 1
2.1 問題の設定 …… 1
2.2 加速器の高周波システム …… 2
2.3 制御の原理 …… 3
2.4 外部特性 …… 6
2.5 制御信号の性質 …… 7
2.5.1 高周波信号エネルギーの関係 …… 7
2.5.2 変調の規則 …… 9
2.5.3 同調特性 …… 9
2.6 要　約 …… 10
3. 最適化のための一般則 …… 10
4. 高周波信号の決定 …… 12
5. 加速チャンネルの特性 …… 16
6. 結　論 …… 17
参考文献 …… 19
付録1. 空洞中の電磁場の任意な励起の詳細な解析 …… 21
A1.1 電気力学的集合の性質 …… 21
A1.2 励　振 …… 22
A1.3 ウォールロス …… 23
付録2. …… 26
付録3. …… 26
付録4. …… 27
付録5. …… 28
付録6. …… 29

1. Introduction

IFMIF high-duty-factor deuteron linac main specifications are 40 MeV energy and 125 mA beam intensity with pulse operating condition at forcing into continuous-wave operation, [1]. These lead to a need for excellent control of the accelerating fields to obtain the specified high-quality output beam characteristics and to minimize the possibility of the beam loss and the resulting activation, so that the effective RF control is one of the key issues for the linac implementation [2].

Electrodynamics of the high-duty-factor linacs is substantially different from the processes in a few-cells resonator of the ring resonator accelerators, where the beamloading effect of the well-bunched beam is slow varying at the synchrotron frequency, [3,4]. The well-developed [5,6] complex amplitudes (phasor) approximate method assumes a slow variation of amplitude and phase for the field in the form of the single harmonic. The method is exact only for invariable single harmonic and is inadequate for the rigorous analysis of the linac's real transient processes. In addition, the conventional equivalent circuit model for the beamloaded resonator should contain nonlinear elements [7] even at the approximation [5,6]. So the merits of powerful linear circuit methods are disappeared and complete consideration of external properties of the linac's resonator is required.

The present method is based on in-depth analysis of the transient beam excitation of the resonator. After setting of the problem in sec.2, this analysis at the directional selective coupling RF system [8] application allowed to form basic idea for the control, to define the beamloaded resonator external characteristics, to determine the control signal modulation and its possible optimization. General results for optimization are obtained in sec.3, and the optimized RF control signal with the main RF system parameters are completely determined for IFMIF RFQ in sec.4. The excited field carries the beam dynamic's information, and the total characteristics of the accelerating channel are also defined by optimization results in sec.5. The bases for the analysis are obtained in Appendix 1, where the resonator field is considered in time domain for arbitrary excitations.

2. RF general characteristics

2.1 Setting of the problem

The resonant accelerator design usually employs the single mode principle that assumes the single-harmonic time dependence of the electric field,

$$e_1(t) = A\cos(\omega_0 t + \varphi)\,. \tag{1}$$

The particles dynamics analysis also uses the above field approximation with addition of the gradient (self-Coulomb) field. After all the beam characteristics for the optimized

operating condition are known, the tolerable deviations $\Delta A, \Delta\omega_0, \Delta\varphi$ of the Eq.(1) parameters can be determined. The RF control system design for this operating condition implementation[1] is the main objective of the work.

2.2 Accelerator RF system

Generally, the resonator field is represented in the form of Eq.(65), Appendix 1; the gradient summand is taken into account at the beam dynamics simulation, so the rotational ν-type resonator modes to be analyzed (operating mode is denoted by index 1). The dimensionless time functions $e_\nu(t), h_\nu(t)$ are defined by Eq.(80) in Appendix 1 at $\vec{m}(\vec{R},t) = 0$:

$$\begin{cases} (1+\frac{1}{Q_\nu})h''_\nu + \frac{\omega_\nu}{Q_\nu}h'_\nu + \omega_\nu^2 h_\nu = \frac{-\omega_\nu}{W_\nu}(In_L + In_B)\,, \\ In_L(t) = \int\limits_V \left(\vec{E}_\nu(\vec{R}), \vec{j}_L(\vec{R},t)\right) dV\,, \quad In_B(t) = \int\limits_V \left(\vec{E}_\nu(\vec{R}), \vec{j}_B(\vec{R},t)\right) dv\,, \\ e_\nu = \frac{1}{\omega_\nu}(1+\frac{1}{Q_\nu})h'_\nu + \frac{1}{Q_\nu}h_\nu\,; \end{cases} \tag{2}$$

where $\vec{j}_B$ and $\vec{j}_L$ are the beam and the coupling elements current densities respectively. The use of grid-control device (e.g., tetrode) for RF source output stages gives the possibility to synthesize RF signal in relatively wide band (the typical bandwidths are $1\ldots5\%$). In addition, the high linearity in the transfer function[2] allow to form all control signals at low power level. In this case the application of directional selective coupling principle [8] puts away the problem of undesirable modes excitation by the relatively wide-band signal, because for any signal $In_L = 0\ \forall\nu \neq 1$ and at the beam excitation the undesirable mode quality factors $Q_\nu|_{\nu\neq1}$ will be lowered, so the operating mode processes present the main interest.

Assuming the operating mode magnetic field does not contain the low frequencies components and $Q_1 \gg 1$, the last equations take the form

$$\begin{cases} h''_1 + \frac{\omega_r}{Q_r}h'_1 + \omega_r^2 h_1 = \frac{-\omega_r}{W_1}(In_L + In_B)\,, \\ e_1 = h'_1\frac{1}{\omega_r}\,; \end{cases} \tag{3}$$

where $\omega_r = \omega_1(1+\frac{1}{Q_1})^{-\frac{1}{2}}$, $Q_r = \sqrt{1+Q_1^2}$. To define In_L the linear RF feed system can be presented by the equivalent current source I_s with active output impedance ρ in the reference plane of each coupling loop, Fig. 1, and integration over the loop conductor

[1] It is better to know the admissible speeds $\frac{d\Delta A}{dt}, \frac{d\Delta\omega_0}{dt}, \frac{d\Delta\varphi}{dt}$ or other admissible time-domain characteristics for the complete design; however, such an information seems to be inaccessible now.

[2] These are noteworthy differences from a klystron, and the tetrode operating condition can be corrected under DC control for its optimal efficiency obtaining at processing of the input signals.

length l_u and transverse cross-section S_c yields [3]

$$In_L = \int_{l_u}\int_{S_c}(\vec{E}_1, \vec{j}_L)dS_c dl = I_L \int_{l_u}(\vec{E}_1, \vec{dl}) = I_L \int_{S_l}(\mathrm{rot}\vec{E}_1, \vec{dS}) = I_L \cdot [-\omega_1 \mu \int_{S_l}(\vec{H}_1, \vec{dS})],$$

where S_l is the loop space.

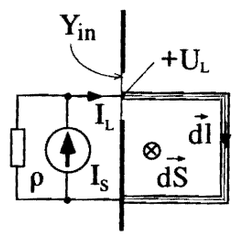

Fig. 1. Equivalent circuit of RF feed system in the reference plane.

As far as $I_S = I_L + U_L/\rho$, where the induced loop voltage

$$U_L = -\int_{l_u}(e_1 \cdot \vec{E}_1, \vec{dl}) = e_1 \cdot \omega_1 \mu \int_{S_l}(\vec{H}_1, \vec{dS}),$$

set (3) for the m identical loops feeding case takes the form

$$\begin{cases} h_1'' + \dfrac{\omega_r}{Q_L}h_1' + \omega_r^2 h_1 = S_s(t) + V(t), \\ e_1 = h_1' \dfrac{1}{\omega_r}. \end{cases} \tag{4}$$

The loaded quality factor of the operating mode Q_L is determined by

$$\frac{\omega_r}{Q_r} + \frac{m}{\rho W_1}(\omega_r \mu K_l)^2 = \frac{\omega_r}{Q_L}, \qquad K_l = \int_{S_l}(\vec{H}_1, \vec{dS}); \tag{5}$$

the beam excitation and RF source signals are

$$V(t) = \frac{-\omega_r}{W_1}\int_V \left(\vec{E}_1(\vec{R}), \vec{j}_B(\vec{R}, t)\right) dv, \qquad S_s(t) = I_S(t) \cdot \frac{\omega_r^2 \mu m}{W_1} K_l; \tag{6}$$

and the input conductance is

$$Y_{in} = \frac{I_L}{U_L} = \frac{h_1'' + \frac{\omega_r}{Q_r}h_1' + \omega_r^2 h_1 - V(t)}{h_1'} \cdot \frac{W_1}{m\,(\omega_r \mu K_l)^2}. \tag{7}$$

2.3 Control principles

Without loss of generality, consider the beam with as much as desired but finite duration τ_{in},[4] which leading front (Fig. 2) enters the resonator at $t = 0$, so $V(t) = 0$ at $t \leq 0$. Also

[3] The constant loop current I_L distribution over the loop length and $\vec{E}_1$ independence over S_c are assumed. The countour is closed by adding the path on the resonator wall where $(\vec{E}_1, \vec{dl}) = 0$, Stokes theorem is applied with the use of the mode field spatial distribution definition (Eq.(60) in Appendix 1).

[4] For the real T_B duration pulses operating condition it will be enough to add to the final result the same T_B-delayed one with opposite sign since $\tau_{in} \gg T_B$.

for the general case the source signal can be presented as $S_s(t) = S_-(t) + S(t)$, where $S_-(t)$ was started before $t = 0$ and sets up[5] the specified by Eq.(1) field,

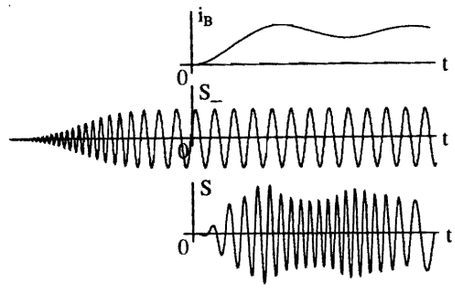

Fig. 2. Beam current i_B in the resonator input with the forestalling S_- and compensative S control signals.

whereas $S(t)$ starts simultaneously with the leading front at $t = 0$. Then, the linear form of Eq.(4) yields the condition for $S(t)$ synthesis: the solution h of

$$h'' + \frac{\omega_r}{Q_L}h' + \omega_r^2 h = S(t) + V(t) \quad \text{at} \quad h''(0) = h'(0) = h(0) = 0 \tag{8}$$

must be zero for $t > 0$ in the ideal $S(t)$ case and the control system must hold up variations of $V(t) + S(t) + S_-(t)|_{t>0}$ in required limits.

Trivial solution for ideal signal $S(t) = -V(t)$ may be unrealizable since the limited bandwidth of the source, in addition this solution is far from the best in the meaning of the required RF energy.

To reveal the physical sense of $V(\omega)$ spectrum under Fourier transform $\mathbf{F}\{i\omega\}$ application, consider the energy variation $\mathcal{E}_a$ of the beam particle a with charge $\overline{e}$, which moves on $\vec{r_a}(t)$ trajectory with $\vec{v_a}(t)$ velocity in a mode field $\vec{E} = e_\nu(t)\cdot\vec{E}_\nu(\vec{R})$, [9]:

$$\frac{d\mathcal{E}_a}{dt} = \overline{e}\left(\vec{v_a}(t), \vec{E}\right) = e_\nu(t)\cdot\overline{e}\left(\vec{v_a}(t), \vec{E}_\nu(\vec{r_a}(t))\right). \tag{9}$$

As far as the beam current is formed by all the particles: $\vec{j}_B(\vec{R}, t) = \sum_a \overline{e}\vec{v_a}(t)\delta(\vec{R} - \vec{r_a}(t))$, the integral in Eq.(2) takes the form

$$In_B(t) = \sum_a \begin{cases} \overline{e}\left(\vec{v_a}(t), \vec{E}_\nu(\vec{r_a}(t))\right) & \text{if } a \text{ particle is in the resonator} \\ 0 & \text{otherwise}. \end{cases} \tag{10}$$

Comparison of the Eq.(9),(10) yields

$$e_\nu(t)\cdot In_B(t) = \sum_a \frac{d\mathcal{E}_a}{dt}, \tag{11}$$

where the extension of $\mathcal{E}_a(t)$ function definition on the constant value (which is equal to the final $\mathcal{E}_a$ energy from the time of leaving the resonator or from the instant of the loss on the wall) eliminates the bivariant condition. The last result is exact for any mode or

[5]The synthesis of $S_-(t)$ for RF source predictive energy minimization at $t < 0$ will be considered separately.

for any resonator without any assumptions on the particles velocities range, for different particle charges also. Thus, the operating mode beam excitation signal $V(t)$ satisfies the equation

$$A\cos(\omega_0 t+\varphi)\cdot V(t) = \frac{-\omega_r}{W_1}\sum_a \frac{d\mathcal{E}_a}{dt} = F(t)\,, \tag{12}$$

where the total energy derivative dependence, denoted by $F(t)$, and its spectrum $F(\omega)$ are known functions, sec. 2.1. The spectrum $V(\omega)$ transformation according to Eq.(12) is presented on Fig. 3. As far as ω_0 is near ω_r, and Fourier operator of the Eq.(8) left-hand side has the narrow bandwidth (the loaded resonator frequency characteristic), the desirable zero solution of Eq.(8) with required precision is obtained at $V(\omega)$ compensation by $S(\omega)$ only in $[\omega_L, \omega_h]$ band in ω_0 vicinity, Fig. 3a. Exact values of ω_L and ω_h are determined by the concrete structure of the control system under admissible $\Delta A, \Delta\omega_0, \Delta\varphi$ deviations.

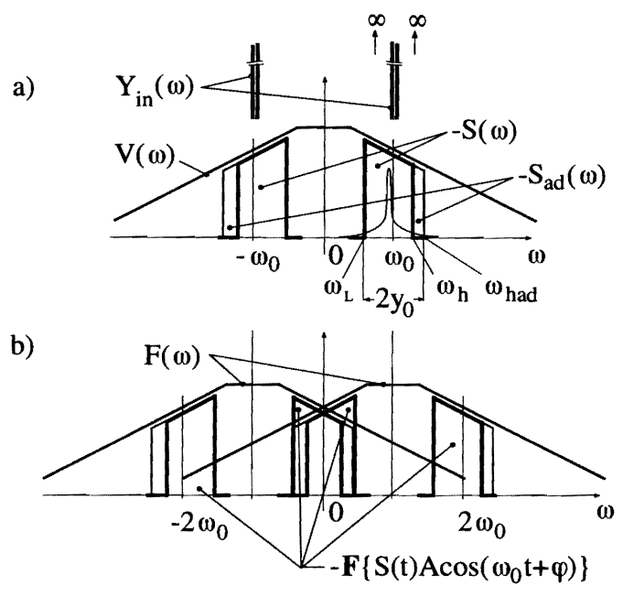

Fig. 3. a) Input conductance $Y_{in}(\omega)$, beam excitation V and compensative signal S spectrums, b) the spectrums transformation in compliance with Eq.(12).

The $[\omega_L, \omega_h]$ width is expected to be less than hundred bandwidths of the loaded resonator, so that S signal remains narrow-band. However, the appealing possibility to use the principle of $F(\omega)$ compensation by $\mathbf{F}\{S(t)A\cos(\omega_0 t+\varphi)\}$ only in the low frequency band (Fig. 3b) for S synthesis and for the control system design is inconsistent because of the "mirror channel" effects[6].

[6] Well-known effect at heterodyne receiving of radio-signals, e.g., consider one of the V components in the form $V = \cos((\omega_0+\varpi)t+\gamma+\varphi)$, $\varpi \ll \omega_0$, and the signal $S = -\cos(\varpi t+\gamma)\cos(\omega_0 t+\varphi) = -\frac{1}{2}[\cos((\omega_0+\varpi)t+\gamma+\varphi)+\cos((\omega_0-\varpi)t-\gamma+\varphi)]$: the compensation is absent. However, the spectrums $\mathbf{F}\{S(t)A\cos(\omega_0 t+\varphi)\} = \frac{-\pi A}{2}[e^{-i\gamma}\delta(\omega+\varpi)+e^{i\gamma}\delta(\omega-\varpi)]+\mathrm{HF1}$ and $F(\omega) = \frac{\pi A}{2}[e^{-i\gamma}\delta(\omega+\varpi)+e^{i\gamma}\delta(\omega-\varpi)]+\mathrm{HF2}$, where HF1, 2 are the high frequency components, give zero sum in the low frequency band.

2.4 External characteristics

At the obtained zero solution of Eq.(8) the second Eq.(4) gives $h_1 = A\frac{\omega_r}{\omega_0}\sin(\omega_0 t+\varphi)$ since $e_1(t)$ has Eq.(1) form, and the frequency domain conductance is defined under Fourier images consideration for Eq.(3)-(7),

$$Y_{in}(\omega) = \left(\frac{\omega_r(1+i\xi)}{Q_r} - \frac{V(\omega)}{A\pi\omega_r[e^{i\varphi}\delta(\omega-\omega_0)+e^{-i\varphi}\delta(\omega+\omega_0)]}\right)\cdot\frac{W_1}{m\,(\omega_r\mu K_l)^2}, \qquad (13)$$

where $\xi = \frac{\omega^2-\omega_r^2}{\omega\omega_r}Q_r$ is the generalized deviation of the resonator. The conductance takes finite values only at $\omega = \pm\omega_0$, shown schematically on Fig. 3a, since the I_s source (Fig. 1) spectrum width is finite, while the resonator field contains single harmonic and the induced voltage U_L is different from zero only at ω_0 frequency. So, at $\omega \neq \omega_0$ all the source power will be reflected and absorbed in matching devices[7] (decoupled port of the circulator), and this property of the reflectance can be used to provide support signals for the control system.

The value on ω_0 is determined by selecting the component $V_0\pi[e^{iv_0}\delta(\omega-\omega_0)+e^{-iv_0}\delta(\omega+\omega_0)]$ [8] in the beam excitation signal,

$$Y_{in}(\omega_0) = \left(\frac{\omega_r(1+i\xi_0)}{Q_r} - \frac{V_0}{A\omega_r}e^{i(v_0-\varphi)}\right)\cdot\frac{W_1}{m\,(\omega_r\mu K_l)^2}. \qquad (14)$$

For bunched beam the $(v_0-\varphi)$ parameter has the meaning of synchronous (equilibrium) phase, and since in the majority of cases $v_0-\varphi \neq 0$, the resonator must be tuned in accordance with

$$\omega_0^2-\omega_r^2 = \frac{\omega_0}{\omega_r}\cdot\frac{V_0}{A}\sin(v_0-\varphi) \qquad (15)$$

for $\Im\{Y_{in}(\omega_0)\}=0$ resonance condition; therewith RF source matching will be realized at

$$\frac{1}{\rho} = \Re\{Y_{in}(\omega_0)\} = \left(\frac{\omega_r}{Q_r} - \frac{V_0}{A\omega_r}\cos(v_0-\varphi)\right)\cdot\frac{W_1}{m\,(\omega_r\mu K_l)^2}. \qquad (16)$$

It is worthy of note that the same $Y_{in}(\omega_0)$ value is obtained for the resonator without the beam ($V_0 = 0$ in Eq.(14)) but with new resonant frequency ω_{eq} and new unloaded quality factor Q_{eq}:

$$\omega_{eq} = \sqrt{\omega_r^2+\frac{\omega_0}{\omega_r}\cdot\frac{V_0}{A}\sin(v_0-\varphi)}, \qquad Q_{eq} = \frac{\sqrt{\omega_r^2+\frac{\omega_0}{\omega_r}\cdot\frac{V_0}{A}\sin(v_0-\varphi)}}{\frac{\omega_r}{Q_r}-\frac{V_0}{A\omega_r}\cos(v_0-\varphi)}. \qquad (17)$$

Usually, the real coupling device properties remain constant with frequency in vastly wider band than $[\omega_L, \omega_h]$ (Fig. 3a) even for much more complicated than Fig. 1 model devices.

[7] The effect can be interpreted as the following: without signal S the beam excited the resonator field in the wide band and some beam's energy was loosed in the resonator walls; with the signal the above energy losses disappear since the field is single harmonic, but this energy of S is loosed in the matching devices.

[8] This form assumes continuous extension of the harmonic onto $t \in (-\infty; +\infty)$ that does not give any distortions for the following results in the finite time interval of $V(t)$ definition because the second term in Eq.(13), as well as in Eq.(7), presents only the ratio of time functions.

Because of this, nothing more than inconsistency between the real and determined by the second Eq.(5) coefficients, some indeterminacy of the reference plane (Fig. 1) position, and the resonant frequency shift due to the device elements reactance take place in the real case. The last expressions do not contain these factors and can be used for precise tuning of the resonator.

2.5 Control signal properties

The extension of $\mathcal{E}_a(t)$ definition delivers $\int\limits_{-\infty}^{+\infty} |\sum\limits_a \mathcal{E}_a| dt > \infty$, so that analysis of the Eq.(12) integral $\mathbf{F}\left\{\sum\limits_a \mathcal{E}_a(t)\right\}$ is hampered since the Fourier image may be nonexistent. For rigorous treatment consider the functions $\mathcal{E}_{ac}(t) = \mathcal{E}_a(t) - \mathcal{E}_a(t - T_c)$, $T_c > 0$; $F_c(t) = F(t) - F(t - T_c)$ and also $\int\limits_{-\infty}^{+\infty} F_c(t)dt = 0$. These functions integration yields

$$\mathbf{F}\left\{\frac{-\omega_r}{W_1}\sum_a \mathcal{E}_{ac}(t)\right\} = F(\omega)\cdot\frac{1 - e^{-i\omega T_c}}{i\omega},$$

and

$$\frac{\omega_r^2}{W_1^2}\int\limits_0^{\infty}\left(\sum_a \mathcal{E}_{ac}(t)\right)^2 dt = \frac{1}{2\pi}\int\limits_{-\infty}^{+\infty} |\,F(\omega)\,|^2\cdot\left|T_c\frac{\sin\frac{\omega T_c}{2}}{\frac{\omega T_c}{2}}\right|^2 d\omega\,.$$

The second factor in the integral over ω brings out the $|\,F(\omega)\,|^2$ filtering in $\approx 1/T_c$ bandwidth. The a particle is inside the resonator at $t \in [\tau_{ai}, \tau_{ao}]$; for $\max\{\tau_{ao} - \tau_{ai}\} \ll T_c < \tau_{in}$ with τ_{in} increase the left-hand side integral approximates to $\tau_{in}\cdot\left(\sum\limits_a \mathcal{E}_a(T_c)\right)^2$, and for $T_c \gg \tau_{in}$ with T_c increase it approximates to $T_c\cdot\left(\sum\limits_a \mathcal{E}_a(\tau_{ao})\right)^2$, but τ_{in}, T_c must remain finite. Nevertheless, the Eq.(12) integration by parts result for spectrum

$$F(\omega) = \frac{-\omega_r}{W_1}\sum_a\left(\mathcal{E}_a(\tau_{ao})e^{-i\omega\tau_{ao}} + i\omega\int\limits_{\tau_{ai}}^{\tau_{ao}}\mathcal{E}_a(t)e^{-i\omega t}dt\right) \tag{18}$$

at $\omega = 0$ gives

$$F(0) = \frac{-\omega_r}{W_1}\sum_a \mathcal{E}_a(\tau_{ao})\,. \tag{19}$$

Thus, the value of $\int |\,F(\omega)\,|^2\,d\omega$ over the low frequency band may be taken as preassigned, since it presents the main characteristics of the accelerated beam.

2.5.1 RF signal energy relations

To analyze the required $S(\omega)$ characteristics consider the symmetrical band signal $S_0(\omega) = S(\omega) + S_{ad}(\omega)$, as shown on Fig. 3; in the general case

$$S_0(\omega) = C_0(\omega - \omega_0)e^{i\alpha(\omega-\omega_0)} + C_0(-\omega - \omega_0)e^{-i\alpha(-\omega-\omega_0)}\,, \tag{20}$$

where modulus $C_0(y)$ and phase $\alpha(y)$ are defined in symmetrical interval $y \in [-y_0, +y_0]$, $y_0 = \omega_0 - \omega_L = \omega_{had} - \omega_0$. Now the spectrum

$$\mathbf{F}\{-S_0(t)\cdot A\cos(\omega_0 t + \varphi)\} = \frac{-A}{2}[e^{i\varphi}\left(C_0(\omega - 2\omega_0)e^{i\alpha(\omega-2\omega_0)} + C_0(-\omega)e^{-i\alpha(-\omega)}\right) + e^{-i\varphi}\left(C_0(\omega)e^{i\alpha(\omega)} + C_0(-\omega - 2\omega_0)e^{-i\alpha(-\omega-2\omega_0)}\right)]$$

coincidence with $F(\omega)$ in the low frequency band $\omega \in [-y_0, +y_0]$, Fig. 3b, at the squared modulus integration over $[-y_0, +y_0]$ yields

$$\mathrm{E}\pi = \mathrm{E}_0\pi - \int_{y_b}^{y_0} C_0^2(\omega)d\omega\,, \tag{21}$$

where $\mathrm{E} = \frac{1}{\pi}\int_0^\infty |S(\omega)|^2\,d\omega$ is the S signal energy, $y_b = \omega_h - \omega_0$, and the S_0 energy $\mathrm{E}_0 = \frac{1}{\pi}\int_{-y_0}^{y_0} C_0(\omega)^2 d\omega$ obeys the equation

$$\mathrm{E}_0\pi = \frac{2\int_{-y_0}^{y_0} |F(\omega)|^2\,d\omega}{A^2} - \int_{-y_0}^{y_0} C_0(\omega)C_0(-\omega)\cos(2\varphi - \alpha(-\omega) - \alpha(\omega))d\omega\,. \tag{22}$$

The first term value is prescribed, and for any $C_0(y)$ functions the minimal E_0, E energies will be delivered at

$$2\varphi - \alpha(-\omega) - \alpha(\omega) = 0\ (\pm 2\pi n)\,. \tag{23}$$

Therewith the application of Cauchy-Schwarz inequality for the second term in Eq.(22) yields

$$2\mathrm{E}_0\pi \geq \frac{2\int_{-y_0}^{y_0} |F(\omega)|^2\,d\omega}{A^2}\,,$$

and the further minimization of E_0, E will be obtained when the latter turns into equality, i.e., at

$$C_0(\omega) = C_0(-\omega)\,. \tag{24}$$

The Eq.(23,24) interpretation is the following: for prescribed $\int_{-y_0}^{y_0} |F(\omega)|^2\,d\omega/A^2$ value the minimal RF energy of S signal will be obtained if $V(\omega)$ spectrum in $[\omega_L, \omega_{had}]$ band is the spectrum of an amplitude modulated signal only. Usually the resonant frequency deviation (Eq.(15)) is commensurable with the resonator bandwidth while the required for compensation the symmetrical refer ω_r band $[\omega_L, \omega_h]$ is expected to be not smaller than several tens of the bandwidths, so that $y_b \approx y_0$ and the Eq.(21) second term is much smaller than the first one. Because of this, the further $S(\omega)$ analysis will be conducted for wider than required but symmetrical refer ω_0 band: $\omega_h = \omega_{had}$, that increase the control accuracy but deliver insignificant loss in RF energy meaning[9]. Thus, the engineering synthesis of the optimal signal is the simplest since it is only the amplitude modulated.

[9]Final result can be corrected by simplest filtering to avoid this assumption.

2.5.2 Modulation laws

In the general case the signal can be presented in the quadrature form

$$S(t) = A_0(t)\cdot\cos(\omega_0 t + \varphi) + B_0(t)\cdot\sin(\omega_0 t + \varphi)\,, \tag{25}$$

where $A_0(\omega), B_0(\omega)$ spectrums are defined in $\omega \in [-y_0, +y_0]$ band. The required compensation of $F(\omega)$ by $\mathbf{F}\{S(t)\cdot A\cos(\omega_0 t + \varphi)\}$ not only in the low frequency band $F_0(\omega) = F(\omega)|_{\omega\in[-y_0,+y_0]}$, but also in the $F_{+2}(\omega) = F(\omega)|_{\omega\in[2\omega_0-y_0,2\omega_0+y_0]}$ with $F_{-2}(\omega) = F(\omega)|_{\omega\in[-2\omega_0-y_0,-2\omega_0+y_0]}$ bands gives

$$A_0(\omega) = \frac{-2}{A}F_0(\omega)\,,$$

$$A_0(\omega-2\omega_0)-iB_0(\omega-2\omega_0)=\frac{-4e^{-i2\varphi}}{A}F_{+2}(\omega)\,,\quad A_0(\omega+2\omega_0)+iB_0(\omega+2\omega_0)=\frac{-4e^{i2\varphi}}{A}F_{-2}(\omega)\,;$$

the existence of these three equations proves the realizability of $A_0(t), B_0(t)$ and

$$B_0(\omega) = \frac{2i}{A}\left(F_0(\omega) - 2F_{+2}(\omega + 2\omega_0)e^{-i2\varphi}\right).$$

Thus, returning to Eq.(25), the required control signal $S(t) = A_{mod}(t)\cos(\omega_0 t + \varphi + \Phi(t))$ in the general case contains the amplitude modulation

$$A_{mod}(t) = \frac{2}{A}\sqrt{(\mathbf{F}^{-1}\{F_0(\omega)\})^2 + (\mathbf{F}^{-1}\{i(F_0(\omega) - 2F_{+2}(\omega + 2\omega_0)e^{-i2\varphi})\})^2} \tag{26}$$

and the phase modulation

$$\Phi(t) = \arctan\left(\frac{\mathbf{F}^{-1}\{i(F_0(\omega) - 2F_{+2}(\omega + 2\omega_0)e^{-i2\varphi})\}}{\mathbf{F}^{-1}\{F_0(\omega)\}}\right), \tag{27}$$

where $F(\omega)$ spectrum is defined by Eq.(18) at the determined $\mathcal{E}_a(t)$. The energy of the signal will be minimal under fulfilment of the conditions

$$\Re\left\{\frac{2F_{+2}(\omega + 2\omega_0)e^{-i2\varphi}}{F_0(\omega)}\right\} = 1\,,\qquad \Im\left\{\frac{2F_{+2}(\omega + 2\omega_0)e^{-i2\varphi}}{F_0(\omega)}\right\} = \mathrm{const}(\omega)\,; \tag{28}$$

in this case the phase modulation will be absent.

2.5.3 Tuning characteristics

The condition at ω_0 harmonic selecting for (14) form is zero correlation of the residual $V(t) - V_0\cos(\omega_0 t + v_0)$ signal with $\cos(\omega_0 t + \varphi)$ in the finite interval of $V(t)$ definition, since $h_1' \propto \cos(\omega_0 t + \varphi)$, and with the any other phases ω_0 harmonics also:

$$\int_0^{\tau_o} ([V(t) - V_0\cos(\omega_0 t + v_0)]\cdot\cos(\omega_0 t + \varphi))\,dt = 0 \quad \forall\varphi\,,$$

where $V_0 \cos(\omega_0 t + v_0)$ presents chosen harmonic in $t \in [0; \tau_o]$ interval – the last particle leaves the resonator at $t = \tau_o$, evidently $\tau_o \geq \tau_{in} + \min\{\tau_{ao} - \tau_{ai}\}$. The condition is fulfilled under the quadrature components equality

$$\begin{cases} \int\limits_0^{\tau_o} V(t)\cos(\omega_0 t)dt &= \int\limits_0^{\tau_o} V_0 \cos(\omega_0 t)\cos(\omega_0 t + v_0)dt\,, \\ \int\limits_0^{\tau_o} V(t)\sin(\omega_0 t)dt &= \int\limits_0^{\tau_o} V_0 \sin(\omega_0 t)\cos(\omega_0 t + v_0)dt\,; \end{cases}$$

and at the satisfiable with any finite precision $\omega_0 \tau_o \gg 1$ it yields

$$v_0 = \arg\left(V(\omega_0)\right)\,, \quad V_0 = \frac{2}{\tau_o}\left|V(\omega_0)\right|. \tag{29}$$

The characteristics on ω_0 frequency for Eq.(14-17) can be expressed in $F(\omega)$ terms with the use of Eq.(25) since $V(\omega_0) = -S(\omega_0)$:

$$V_0 = \frac{4}{A\tau_o}\left|F_{+2}(2\omega_0)\right|\,, \quad v_0 = \arg\left(F_{+2}(2\omega_0)\right) - \varphi\,, \quad V_0\cos(v_0 - \varphi) = \frac{2F_0(0)}{A\tau_o}. \tag{30}$$

2.6 Resume

1. Basic idea for the control and the condition (Eq.(8)) for state equation are obtained in sec.2.3.
2. Accelerating resonator external characteristics for RF feed system design are defined in sec.2.4, Eq.(17) determine beam's equivalent for the system precise tuning.
3. The reflected wave properties, derived from Eq.(13): full reflection at $\omega \neq \omega_0$ with zero reflection on $\omega = \omega_0$ form the possible support for the control.
4. Spectrum $F(\omega)$ completely determines the control signal (Eq.(26,27)) and the tuning characteristics (Eq.(30,17)). This spectrum is defined from dynamic's simulation by scalar functions $\mathcal{E}_a(t)$, Eq.(18).
5. Optimal control signal delivers minimum of RF source energy, the signal is simple for realization since it is only the amplitude modulated. The optimum conditions (Eq.(28)) are also expressed in terms of $F(\omega)$ spectrum.

The conditions (Eq.(28)) are used for RF system optimization in the following section.

3. General for optimization

Assuming the required signal $S_s(t)$ is synthesized and the control system operates ideal, so that resonator field time dependence has Eq.(1) form, the beam particles energy variation will be $T = 2\pi/\omega_0$ periodic [10]

$$\sum_a \mathcal{E}_a(t) = \sum_{n=1}^{N} \mathcal{E}_0\Big(t - (n-1)T\Big)\,, \tag{31}$$

[10] The difference between the self-Coulomb field for the leading front particles and for the inside the beam ones is disregarded now, however it can be taken into account at final simulation.

where NT ($N \gg 1$) is the beam duration; $\mathcal{E}_0(t)$ is the total energy variation of the particles that enter the resonator at $t \in [0, T]$, the last particle from these leaves the resonator at $t = KT+\zeta$ ($K < N$, $0 \le \zeta < T$), and $\mathcal{E}_0(t)|_{t \ge KT+\zeta} = \mathcal{E}_{out} = \mathrm{const}(t)$. Fourier transform of the principal function $F(t)$, defined by Eq.(12), is

$$F(\omega) = \frac{-\omega_r}{W_1} D(\omega) P(\omega), \quad P(\omega) = \sum_{n=1}^{N} e^{-i\omega(n-1)T} = \frac{\sin(\frac{\pi\omega}{\omega_0}N)}{\sin(\frac{\pi\omega}{\omega_0})} e^{-i\frac{\pi\omega}{\omega_0}(N-1)}, \tag{32}$$

where $D(t) = \dfrac{d\mathcal{E}_0(t)}{dt}$ and also $D(t)|_{t \notin (0, KT+\zeta)} = 0$,

$$D(\omega) = \mathcal{E}_{out} e^{-i\omega(KT+\zeta)} + i\omega \int_0^{KT+\zeta} \mathcal{E}_0(t) e^{-i\omega t} dt. \tag{33}$$

The $P(\omega)$ function brings out $|D(\omega)|^2$ filtering at determination of the prescribed value under RF optimization (sec.2.5); according to Appendix 2 this prescribed value

$$\frac{1}{A^2} \int_{-y_0}^{y_0} |F(\omega)|^2 \, d\omega = \frac{\mathcal{E}_{out}^2 N}{A^2} \cdot \frac{\omega_0 \omega_r^2}{W_1^2} \tag{34}$$

even for rather wide band ($y_0 < \frac{\omega_0}{2}$) case. It includes basic specifications of the accelerated beam for prescribed resonator indeed, but the optimization is essentially restricted from the Eq.(23) condition, because the condition requires the phase θ fixation for the amplitude modulated signal carrier $\propto \cos(\omega_0 t + \theta)$. Nevertheless, comprehensive analysis in Appendix 3 shows that the amplitude modulated signal is optimal at any θ, delivering the global minimum for required energy of the compensative control signal

$$\mathrm{E}_0 \pi = \frac{\int_{-y_0}^{y_0} |F(\omega)|^2 \, d\omega}{A^2 \cos^2(\varphi - \theta)}. \tag{35}$$

With the use of Eq.(32) where $P(\omega + m\omega_0) = P(\omega)$, $m = 0, \pm 1, \pm 2, \ldots$, the optimization conditions (Eq.(28)) take the form

$$\Re\left\{\frac{2D_{+2}(\omega + 2\omega_0)e^{-i2\varphi}}{D_0(\omega)}\right\} = 1, \qquad \Im\left\{\frac{D_{+2}(\omega + 2\omega_0)e^{-i2\varphi}}{D_0(\omega)}\right\} = \mathrm{const}(\omega), \tag{36}$$

where 0 and +2 indexes denote the same frequency bands as for $F(\omega)$ in sec.2.5.2. The solutions are presented by the form

$$D_b(t) = M(t) \cdot \cos(\omega_0 t + \varphi) \cdot \cos(\omega_0 t + \theta), \tag{37}$$

where $M(t)$ spectrum is not wider than $\omega \in (-\omega_0, +\omega_0)$ band but not narrower than $[-y_0, +y_0]$ and θ is some angle; Appendix 4 contains the direct verification. Since the conditions specify $D(\omega)$ (and $F(\omega)$) properties only in (0) and ($\pm 2\omega_0$) bands (Fig.3b), with the other bands excitation the general form is

$$D(t) = M(t) \cdot \cos(\omega_0 t + \varphi) \cdot \cos(\omega_0 t + \theta) + L(t) \cdot \cos(\omega_0 t + \varphi), \tag{38}$$

where $L(t)$ spectrum is not wider than $\omega \in (-\omega_0 + y_0, \omega_0 - y_0)$ band and also $L(t) = M(t) = 0$ at $t \notin (0, KT + \zeta)$.

Thus, returning to Eq.(32) and (12), the general form of the beam excitation signal in the optimized accelerator is

$$V(t) = \frac{-\omega_r}{AW_1}\left(\cos(\omega_0 t + \theta)\sum_{n=1}^{N} M\Big(t-(n-1)T\Big) + \sum_{n=1}^{N} L\Big(t-(n-1)T\Big)\right); \qquad (39)$$

the output energy is defined by $M(\omega)$ function only

$$\mathcal{E}_{out} = D(0) = M(0)\frac{\cos(\varphi-\theta)}{2}, \quad \mathcal{E}^2_{out} = \frac{\cos^2(\varphi-\theta)}{4}\left(\int_0^{KT+\zeta} M(t)dt\right)^2, \qquad (40)$$

since $\mathbf{F}\{L(t)\cos(\omega_0 t + \varphi)\}$ does not contain a constant component.

4. RF signal determination

According to L definition for Eq.(38), the first term in Eq.(39) presents just the (ω_0) band excitation, which is to be compensated by S signal, Fig.3a. As far as $M(t)|_{t\notin(0,KT+\zeta)} = 0$, the envelope will be T periodic

$$\sum_{n=1}^{N} M\Big(t_0-(n-1)T\Big) = \sum_{n=1}^{N} M\Big(t_0+T-(n-1)T\Big) \quad \text{for } t_0 \in [((K-1)T+\zeta), (N-1)T]\,^{11}.$$

However, for sufficiently large t the envelope is to be constant, because at $t \gg KT$ the time-dependence of the first term in Eq.(39) could be obtained from the infinite duration periodic excitation in (ω_0) band, i.e., it would be a single harmonic from the line spectrum. Without loss of generality the $M(t)$ form

$$M(t) = f(t) - f(t-T), \qquad (41)$$

$$f(t)|_{t\le 0} = 0, \; f(t)|_{t\ge(K-1)T+\zeta} = \text{const} = f_s, \; f'((K-1)T+\zeta) = 0, \qquad (42)$$

[11] Integer interval of $M(t)$ definition can be singled out in the form $M(t) = M_1(t) + M_2(t)$,

$$M_1(t) = M(t)|_{t\in[0,KT]}, M_1(t) = 0|_{t\notin[0,KT]} \text{ and } M_2(t) = M(t)|_{t\in(KT,KT+\zeta]}, M_2(t) = 0|_{t\notin(KT,KT+\zeta]}.$$

Evidently, $\sum_{n=1}^{N} M_2\Big(t-(n-1)T\Big)$ function is periodic; and for M_1 sum consider any "m" interval $t = (m+K-1)T + \tau_1$, $0 \le \tau_1 < T$ for $m \in [0, N-K]$, where the limited interval $[0, KT]$ of M_1 definition restricts the number of terms, so that

$$\sum_{n=1}^{N} M_1\Big(t-(n-1)T\Big) = \sum_{n=m}^{m+K-1} M_1\Big(t-nT\Big) = \sum_{n=0}^{K-1} M_1\Big(\tau_1+(K-n-1)T\Big)$$

is the same for any m; selection of the common periodicity range for M_1 and M_2 sums gives the result.

satisfies this condition, the envelope

$$M_\Sigma(t) = \sum_{n=1}^{N} M\Big(t-(n-1)T\Big) = f(t) - f(t-NT)\,, \tag{43}$$

and direct integration of Eq.(41) with the use of Eq.(40) yields the stationary level

$$f_s = \frac{2\mathcal{E}_{out}}{T\cos(\varphi-\theta)}\,. \tag{44}$$

Since the envelope energy in $[-y_0, +y_0]$ band is determined for any $M_\Sigma(t)$ by Eq.(35,34),

$$\frac{1}{4}\int_{-y_0}^{y_0} |\mathbf{F}\,\{f(t)-f(t-NT)\}|^2\,d\omega = \frac{\mathcal{E}_{out}^2 N\omega_0}{\cos^2(\varphi-\theta)}\,, \tag{45}$$

the most complete compensation by S signal will be obtained if the envelope spectrum width will be minimized. The time interval $[0,(K-1)T+\zeta]$ of $M_\Sigma(t)$ variation can be prescribed (e.g., in the RFQ case by the number of cells) and $M_\Sigma(t)$ energy in this interval is defined since the stationary level is determined. That's why the minimal width is achieved by Gauss time-dependence, Appendix 5, and the closely approximating acceptable form is

$$f(t) = f(x\cdot T) = \left[\begin{array}{ll} \dfrac{f_s}{1-e^{-\frac{u^2}{a^2}}}\left(e^{-\frac{(x-u)^2}{a^2}} - e^{-\frac{u^2}{a^2}}\right), & t\in[0,(K-1)T+\zeta] \\ f_s\,, & t\in[(K-1)T+\zeta,\infty)\,; \end{array}\right. \tag{46}$$

where $x = t/T$, $u = (K-1)+\zeta/T$; parameter a still remains free, because for sufficiently large N the low-frequency filtering in Eq.(45) gives the same stationary level f_s for any a, so that the equation yields only

$$N \gg 2K + \frac{\omega_0}{y_0} \tag{47}$$

additional estimation for the N lower bound.

To define the required bandwidth y_0 consider the errors of RF control system. Since the beam excitation signal spectrum is infinite in the any case (the finite time duration signal), the uncompensated signal (Eq.(39)) outside of the $2y_0$ band (Fig. 3.a) excites the field, which is defined by Eq.(4):

$$e_{1un}(t) = \frac{1}{2\pi}\int V(\omega)\frac{Q_L}{\omega_r^2(1+i\xi_L(\omega))}e^{i\omega t}d\omega = -\frac{Q_L}{AW_1 2\pi\omega_r}\cdot$$
$$\int_{y_0}^{gr}\cos(\omega_0 t+\theta+\theta')\cdot|M_\Sigma(\omega)|\left|\frac{e^{i(\arg(M_\Sigma(\omega))+\omega t)}}{1+i\xi_L(\omega+\omega_0)} + \frac{e^{-i(\arg(M_\Sigma(\omega))+\omega t)}}{1+i\xi_L(-\omega+\omega_0)}\right| d\omega\,, \tag{48}$$

where $\xi_L(\omega) = \frac{\omega^2-\omega_r^2}{\omega\omega_r}Q_L$, θ' is argument of the expression under the modulus sign; the integrand function resonance filtration allows to bound the upper integral limit gr and

to neglect the L functions sum contribution. The estimation of the maximal normalized amplitude error from Eq.(48) is

$$(|e_{1un}|/A) \leq$$

$$\frac{b}{2\pi(2+b)\cos(\varphi-\theta)}\int_{y_0}^{gr}\frac{|M_{\Sigma 1}(\omega)|}{f_s}\left[\frac{1}{\sqrt{1+\xi_L^2(\omega+\omega_0)}}+\frac{1}{\sqrt{1+\xi_L^2(\omega_0-\omega)}}\right]d\omega=\frac{e_{1unM}}{A}, \quad (49)$$

where b is the beam power to the cavity power losses ratio, Appendix 6. Here the spectrum modulus $|M_{\Sigma 1}(\omega)| = |\mathbf{F}\{f(t)\}|$ of the leading front dependence from Eq.(43)

$$\frac{|M_{\Sigma 1}(\omega)|}{f_s} = \frac{\left|Ta\frac{\sqrt{\pi}}{2}e^{-\frac{(\omega aT)^2}{4}}\left[\mathrm{erf}(\frac{u}{a}-i\frac{\omega aT}{2})+\mathrm{erf}(i\frac{\omega aT}{2})\right]+\frac{1-e^{i\omega uT}\cdot e^{-\frac{u^2}{a^2}}}{i\omega}\right|}{1-e^{-\frac{u^2}{a^2}}} \quad (50)$$

is used instead of the general $|M_\Sigma(\omega)|$, because the Eq.(48) form excludes the constant component and the maximal $e_{1un}(t)$ value is attained at the commensurable with KT instant[12]; erf – error function. This type error dependence on a and y_0 is presented on Fig. 4 at concrete parameters for IFMIF RFQ [1,10], but Eq.(49) with Eq.(46) analysis shows that the similar dependence takes place in the general case also.

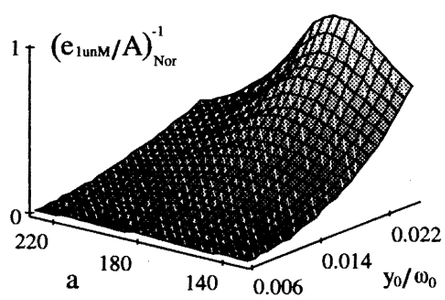

Fig. 4. Reciprocal off-band overshoot (normalized); $b=1.1/1.68$, $u=366$, $Q_r=10^4$ values are taken from [1,10], $\cos(\varphi-\theta)=0.5$.

The second type error is caused by non-ideal compensation inside $2y_0$ band. Assuming the autocontrol system will hold up the difference between V and S signals with random error, which power density spectrum is $w(\omega)$, the mean square field error is

$$\tilde{e}_{1a} = \sqrt{\frac{1}{\pi}\int_{\omega_0-y_0}^{\omega_0+y_0} w(\omega)\left|\frac{Q_L}{\omega_r^2(1+i\xi_L(\omega))}\right|^2 d\omega}.$$

As far as this error increases with the band extension while the off-band overshoot (Eq.(49) and Fig. 4) error decreases, the optimal y_{0m} value in the meaning of the minimal total error $(e_{1unM}+\tilde{e}_{1a})/A$ can be presupposed; however, the normalized $\tilde{e}_{1a}$ value

$$\frac{\tilde{A}}{A} = \frac{1}{A}\sqrt{\frac{1}{\pi}\int_{\omega_0-y_{0m}}^{\omega_0+y_{0m}} w(\omega)\left|\frac{Q_L}{\omega_r^2(1+i\xi_L(\omega))}\right|^2 d\omega} \quad (51)$$

[12]The use of the general Eq.(48) allows to determine this instant, however it is of no interest now.

must be prescribed since this error exists during all the accelerating time interval; therewith the autocontrol system precision Δ_a can be characterized by the normalized power error, because S power is determined by Eq.(35),

$$\Delta_a = \frac{\frac{1}{\pi}\int\limits_{\omega_0-y_{0m}}^{\omega_0+y_{0m}} w(\omega)d\omega\cdot NT}{\mathrm{E}_0}. \tag{52}$$

Assuming the autocontrol error to be white noise (at least in $2y_0$ band), the use of Eq.(49-52) and Appendix 6 parameters yields the equation for the bandwidth values $y_0 = y_{ex}$, which deliver extremums to the total error:

$$\left| a\pi^{\frac{3}{2}} e^{-(\eta_{ex}\pi a)^2}\left[\mathrm{erf}(\frac{u}{a}-i\eta_{ex}\pi a)+\mathrm{erf}(i\eta_{ex}\pi a)\right]+\frac{1-e^{i2\pi\eta_{ex}u}\cdot e^{-\frac{u^2}{a^2}}}{i\eta_{ex}}\right| \left(1-e^{-\frac{u^2}{a^2}}\right)^{-1} =$$

$$\frac{\tilde{A}}{A}\cdot\frac{\pi(2+b)\cos(\varphi-\theta)}{b}\cdot\frac{K^2(1+\eta_{ex})+K^2(1-\eta_{ex})}{[K(1+\eta_{ex})+K(1-\eta_{ex})]\int\limits_{1-\eta_{ex}}^{1+\eta_{ex}} K^2(\eta)d\eta}, \tag{53}$$

where normalized frequency $\eta = \omega/\omega_0$; $\eta_{ex} = y_{ex}/\omega_0$, $r = \omega_r/\omega_0$, the resonant characteristic

$$K(\eta)=\left(1+\left[\frac{\eta^2-r^2}{r\eta}Q_L\right]^2\right)^{-\frac{1}{2}},\ r=1+\gamma,\ \gamma=\sqrt{1+\frac{b^2\tan^2(\varphi-\theta)}{4Q_r^2}}-\left(1+\frac{b\tan(\varphi-\theta)}{2Q_r}\right);$$

the frequency functions in Eq.(48,49,51,53) depend almost not at all on the γ sign[13], so that

$$\gamma \cong \frac{b}{2(2+b)Q_L}\sqrt{\frac{1}{\cos^2(\varphi-\theta)}-1};$$

and Eq.(52) for the total error minimizing bandwidth $\eta_{ex} = \eta_m = y_{0m}/\omega_0$ takes the form

$$\Delta_a = 2\left(\frac{\tilde{A}}{A}\frac{2+b}{b}\cos(\varphi-\theta)\right)^2\left(\frac{\int\limits_{1-\eta_m}^{1+\eta_m} K^2(\eta)d\eta}{2\eta_m}\right)^{-1}. \tag{54}$$

The Eq.(53) has the minimal bandwidth η_m solutions; the number of extremals from Eq.(53) is restricted by determining the range of a from the overshoot dependence (Eq.(49) and Fig.4), and under the reasonable condition

$$\frac{e_{1unM}}{A} < \frac{\tilde{A}}{A}$$

the optimum (a_{opt}, η_{mopt}) can be determined. In Fig. 5 the bandwidth dependencies for $e_{1unM} < 10^{-2}\cdot\tilde{A}$ at $\eta_m < 0.025$, which corresponds to RF source 5% bandwidth limit, are presented for IFMIF RFQ. In reference to unattainable limit of the infinite Gauss front

[13] It would be absolutely correct if the resonant characteristic would be exactly symmetrical refer resonance frequency.

$G_\infty(t)$ (Appendix 5), the use of, e.g., the upper band on Fig. 5 ($a_{opt} \cong 184$) gives the loss 1.019, Fig. 7, so that any other possible solutions could give not more than 2% advantage in the bandwidth value.

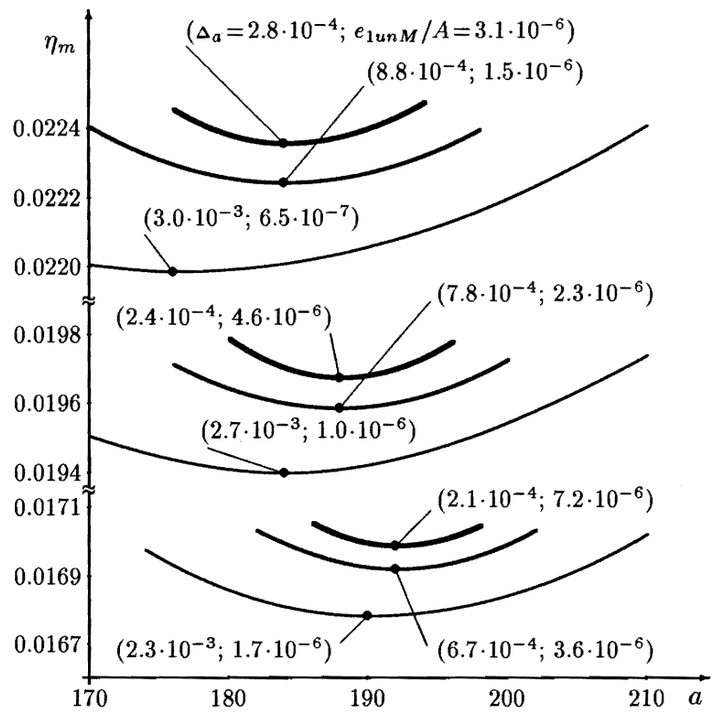

Fig. 5. Minizing bandwidths η_m v.s. parameter a at $\tilde{A}/A = 10^{-3}$, and required control precision Δ_a with off-band overshoot e_{1unM}/A values in optimal points for nominal (—), doubled (—) and half (—) beam currents; $u = 366$, $b = 1.1/1.68$, $Q_r = 10^4$ values are taken from [1,10], $\cos(\varphi - \theta) = 0.5$.

Thus, the required signal is

$$S(\omega) = A\frac{b\omega_r^2}{Q_r\cos(\varphi-\theta)}\mathbf{F}\left\{\frac{f(t)-f(t-NT)}{f_s}\cos(\omega_0 t+\theta)\right\}\Big|_{\omega\in[\omega_0-y_0,\omega_0+y_0]}, \tag{55}$$

where $f(t)$ is defined by Eq.(46),(44) for prescribed $\mathcal{E}_{out}$, N, K, θ values; the optimized a_{opt}, bandwidth value η_{mopt}, and required autocontrol precision are determined by Eq.(53,54) at prescribed random error $\tilde{A}/A$ and maximal tolerable overshoot error e_{1unM}/A in the field magnitude.

5. Accelerating channel characteristics

The use of Eq.(38), where $M(t)$ is already defined (Eq.(41)):

$$M(t) = \left[\begin{array}{ll} f(t)-f(t-T), & t\in[0,(K-1)T+\zeta] \\ f_s - f(t-T), & t\in[(K-1)T+\zeta, KT+\zeta] \\ 0, & t\in[KT+\zeta,\infty), \end{array}\right. \tag{56}$$

determines the energy variation in the accelerating channel

$$\mathcal{E}_0(t) = \frac{\cos(\varphi-\theta)}{2}\int_0^t M(t')dt' + \tag{57}$$

$$\mathbf{F}^{-1}\left\{\frac{1}{4i\omega}\left([M(\omega-2\omega_0)e^{i(\varphi+\theta)}+M(\omega+2\omega_0)e^{-i(\varphi+\theta)}]+2[L(\omega-\omega_0)e^{i\varphi}+L(\omega+\omega_0)e^{-i\varphi}]\right)\right\}.$$

Since the second term presents only the high-frequency oscillations, the energy variation, averaged over the period, is

$$\mathcal{E}_{0A}(t)=\frac{\mathcal{E}_{out}}{1-e^{-(\frac{u}{a})^2}}\left[\begin{array}{ll} \frac{a\sqrt{\pi}}{2}\left[\mathrm{erf}(\frac{x-u}{a})+\mathrm{erf}(\frac{u}{a})\right]-xe^{-(\frac{u}{a})^2}, & x\in[0,1] \\ \frac{a\sqrt{\pi}}{2}\left[\mathrm{erf}(\frac{x-u}{a})+\mathrm{erf}(\frac{x-u-1}{a})\right]-e^{-(\frac{u}{a})^2}, & x\in[1,u] \\ (x-u)-e^{-(\frac{u}{a})^2}-\frac{a\sqrt{\pi}}{2}\mathrm{erf}(\frac{x-u-1}{a}), & x\in[u,u+1] \\ 1-e^{-(\frac{u}{a})^2}, & x\in[u+1,\infty), \end{array}\right. \tag{58}$$

where $x = t/T$, $u = (K-1)+\zeta/T$ as before. Eq.(58) presents rather different $\mathcal{E}_{0A}(t)$ laws for different a, Fig. 6,

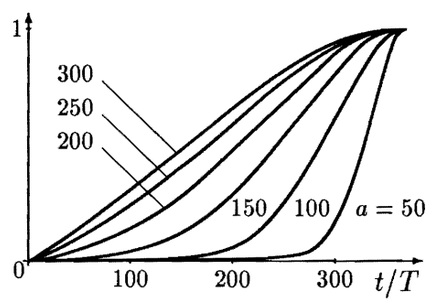

Fig. 6. Normalized averaged energy $\mathcal{E}_{0A}(t)/\mathcal{E}_{out}$ for different a; $u = 367$.

but under the optimized a value the optimal RF field characteristics (sec.4) are obtained with actually insensitive to the beam current variations, Fig. 5, so that the channel with $a = a_{opt}$ is the best.

6. Conclusion

The method of transient beamloading analysis in high-duty-factor linacs gives the solution of key problems at the effective RF control implementation, RF matching realization, and the accelerating structure precise tuning. The developed optimizations provide the following. (1) The beam excitation does not contain phase (and frequency) modulation (Eq.(39)). (2) The required RF source power is minimal for prescribed resonator. (3) RF source bandwidth is minimal for prescribed random error and maximal admissible overshoot error in the field magnitude. The optimization gives only a few percents disadvantage in reference to unrealizable minimal bandwidth limit. (4) RF signal implementation is the simple. (5) The optimized characteristics have only a weak dependence on the beam current deviations.

Concerning the beam dynamics, the energy variation expression contains the single undetermined function ($L(t)$ in Eq.(38)). However, (1) and (5) results allow to presuppose the minimal particle losses at moderate influence of the function, so the dynamic's simulation at the optimized channel with zero value of the function seems to be considered first. The (1-5) extremums are global (in the same meaning as indicated for (3) result), so that the use of the averaged energy variation law, which is maximally correlated with the optimized one ($\mathcal{E}_{0A}(t)$, sec.5), will provide the better results if it can not be implemented exactly; e.g., at RFQ segmentation [11].

Under the control algorithm design, the reflectance property (sec.2.6, 3) can be used and the state-variable control (Kalman filter) seems to be suitable. At the algorithm realization the consideration of the RF support signal processing will give the phase and frequency stability characteristics.

References

(1) Martone M., ed.:"IFMIF Final Conceptual Design Activity Report", ENEA, (1997).

(2) Lynch M. T. et al.:"Proc. of the 1994 International Linac Conf. Tsukuba, Japan", National Laboratory for High Energy Physics (KEK), 454 (1994).

(3) Minty M. G., Siemann R. H.:"Proc. of the 1995 Particle Accelerator Conf.", IEEE Inc., 2907 (1996).

(4) Tighe R., Corredoura P.:"Proc. of the 1995 Particle Accelerator Conf.", IEEE Inc., 2666 (1996).

(5) Pedersen F.: IEEE Trans. Nucl. Sci., NS-32, 2138 (1985).

(6) Wilson P. B.:"AIP Conference Proceedings 87, Fermilab Summer School, 1981", American Institute of Physics, 87, 450 (1982).

(7) Jones R. M. et al.:"1988 Linear Accelerator Conf. Proc. Virginia", CEBAF-Report-89-001, 82 (1989).

(8) Chernogubovsky M. A., Kurchavy A. G., Liverovsky A. K.:"Portable 433 MHz RFQ Linac RF System", Nuc. Instr. Methods Phys. Res.A. , 390, 25 (1997).

(9) Landau L. D., Lifshitz E. M.:"The Classical Theory of Fields" [in Russian], Nauka, Moscow, ch. III (1988).

(10) Sawada K.:"Minutes of the Second IFMIF-CDA Design Integration Workshop", JAERI-Conf 96-012, 187 (1996).

(11) Chernogubovsky M. A., Sugimoto M.:"Conseptual Design of IFMIF Accelerator RF Systems", JAERI-Research 96-064, (1996).

(12) Kisunko G. V.:"Electrodynamics of cavity systems" [in Russian], VKAS, Leningrad, 228 (1949).

(13) Slater J. C.:"Microwave electronics", Van Nostrand, Princeton, N.J., 57-83 (1950).

(14) Wainshtein L. A.:"Electromagnetic waves" [in Russian], Radio i Svyaz, Moscow, ch. IV (1988).

(15) Glock H. W. et al.:"Proc. of the 1993 Particle Accelerator Conf. Washington, USA", IEEE Inc., 623 (1993).

(16) Siebert W. McC. :"Circuits, Signals, and Systems", McGraw-Hill, N.Y., ch. 16 (1986).

(17) Gonorovsky I. S., Demin M. P. :"Radioengineering Circuits and Signals" [in Russian], Radio i Svyaz, Moscow, ch. 2 (1994).

Appendix 1. Detailed Analysis of Resonator Electromagnetic Field at Arbitrary Excitations

The resonator electromagnetic field problem had been considered by various methods; basic principles are stated in [12,13] outstanding works. However, certain of the physical aspects have yet to be considered; more comprehensive treatment is presented.

A1.1 Electrodynamical set properties

Arbitrary ideal (loss-free) resonant cavity field can be expressed by infinite number of rotational and potential eigenfunctions.

The rotational each $\vec{E}^e_\nu, \vec{H}^e_\nu$ (ν-type mode of the resonator) is characterized by eigenfrequency ω_ν and spatial distributions

$$\vec{E}^e_\nu = \cos(\omega_\nu t + \vartheta_\nu)\cdot\vec{E}_\nu(\vec{R}); \qquad \vec{H}^e_\nu = \sin(\omega_\nu t + \vartheta_\nu)\cdot\vec{H}_\nu(\vec{R}), \tag{59}$$

the coordinates dependent spatial distributions $\vec{E}_\nu(\vec{R})$, $\vec{H}_\nu(\vec{R})$ and ω_ν value are the homogeneous Maxwell equations solutions

$$\begin{cases} \mathrm{rot}\vec{H}_\nu(\vec{R}) = -\omega_\nu\varepsilon\vec{E}_\nu(\vec{R}), \\ \mathrm{rot}\vec{E}_\nu(\vec{R}) = -\omega_\nu\mu\vec{H}_\nu(\vec{R}) \end{cases} \tag{60}$$

in the cavity volume V under ideal metal or ideal magnetic boundary conditions or their combinations on the S_r surface, which adjoins the cavity walls but does not include the boundary for homogeneous form of Eq.(60). Phase ϑ_ν in free oscillation expressions (Eq.(59)) is indefinable as well as the amplitude of the spatial distributions. To demonstrate the orthogonality consider the integral $\int\limits_{S_r}\left([\vec{E}_\xi(\vec{R}), \vec{H}_\nu(\vec{R})], d\vec{S}\right)$ and the same for transposed fields; Gauss theorem application with substitutions from Eq.(60) gives

$$\begin{cases} \int\limits_{S_r}\left([\vec{E}_\xi, \vec{H}_\nu], d\vec{S}\right) = -\mu\omega_\xi\int\limits_V\left(\vec{H}_\nu, \vec{H}_\xi\right)dV + \omega_\nu\varepsilon\int\limits_V\left(\vec{E}_\nu, \vec{E}_\xi\right)dV, \\ \int\limits_{S_r}\left([\vec{H}_\xi, \vec{E}_\nu], d\vec{S}\right) = \mu\omega_\nu\int\limits_V\left(\vec{H}_\nu, \vec{H}_\xi\right)dV - \omega_\xi\varepsilon\int\limits_V\left(\vec{E}_\nu, \vec{E}_\xi\right)dV. \end{cases} \tag{61}$$

These surface integrals are zero since ideal boundary conditions and nontrivial solution of the Eq.(61) set for volumetric integrals is possible only at the zero determinant $\varepsilon\mu(\omega_\xi^2 - \omega_\nu^2)$ that yields orthogonality for nondegenerate ($\omega_\xi \neq \omega_\nu$) modes:

$$\left[\begin{array}{ll} \varepsilon\int\limits_V\left(\vec{E}_\nu, \vec{E}_\nu\right)dV = \mu\int\limits_V\left(\vec{H}_\nu, \vec{H}_\nu\right)dV = W_\nu, & \nu = \xi; \\ \int\limits_V\left(\vec{E}_\nu, \vec{E}_\xi\right)dV = \int\limits_V\left(\vec{H}_\nu, \vec{H}_\xi\right)dV = 0, & \nu \neq \xi. \end{array}\right. \tag{62}$$

For degenerate modes it is always possible to use formal Gram-Schmidt orthogonalization process or to prove the orthogonality directly; in the infinite multiplicity degeneration case for 2D or 3D symmetric cavity the basis is formed only by the 2 or 3 perpendicular

oriented modes, these latter are orthogonal in the Eq.(62) sense. In a physical meaning this property (Eq.(62)) reveals the absence of the inter-mode's energy interactions, so all the fields (Eq.(59)) can be in existence independently of one another; W_ν value is in proportion to the ν-mode stored energy of electric or magnetic field; orthonormalized set is constructed under $W_\nu = 1\ \forall\nu$ [14].

In the general case the charge density $\rho(\vec{R},t)$ sets up the potential part of electric field $\vec{E}_{pot} = -\mathrm{grad}\,\varphi(\vec{R},t)$, which is determined by Poisson equation

$$\mathrm{div}\,\mathrm{grad}\,\varphi(\vec{R},t) = -\frac{1}{\varepsilon}\cdot\rho(\vec{R},t) \tag{63}$$

at the same surface boundary conditions. This field can be also presented by the means of dynamical potential eigenfunctions that are determined by scalar wave equation. However, there are no physical meaning of these individual functions in the majority of cases, since these fields have no resonance properties and cannot be in existence separately – e.g., Laplace equation has only trivial solution (summary field of all these functions) for simply connected space in ideal metal cavity. Therefore it is preferable to obtain the Eq.(63) direct closed solution, which must be added to the rotational field.

Completeness of the set is obtained under formal including of similar magnetic potential eigenfunctions also; these functions have no physical meaning since always $\mathrm{div}\vec{H} = 0$ (magnetic charges are absent). Orthogonality of the any potential function to any mode, e.g., $\vec{E}_{gr}$ to $\vec{E}_\nu$ is proved at V-volume integration of the equality $\left(\vec{E}_{gr}, \mathrm{rot}\vec{H}_\nu\right) - \left(\vec{H}_\nu, \mathrm{rot}\vec{E}_{gr}\right) = -\omega_\nu\varepsilon\left(\vec{E}_{gr}, \vec{E}_\nu\right) - \left(\vec{H}_\nu, \mathrm{rot}\vec{E}_{gr}\right)$, which follows immediately from the first equation (60), with taking into account $\mathrm{rot}\vec{E}_{gr} = 0$ and the boundary conditions.

A1.2 Excitation

Electric current with $\vec{j}(\vec{R},t)$ density and the magnetic $\vec{m}(\vec{R},t)$ one set up the resonator field

$$\mathrm{rot}\vec{E} = -\mu\frac{\partial\vec{H}}{\partial t} - \vec{m}(\vec{R},t), \qquad \mathrm{rot}\vec{H} = \varepsilon\frac{\partial\vec{E}}{\partial t} + \vec{j}(\vec{R},t); \tag{64}$$

that can be represented in the form

$$\vec{E} = \sum_\nu e_\nu(t)\cdot\vec{E}_\nu(\vec{R}) + \mathrm{grad}\,\varphi(\vec{R},t), \quad \vec{H} = \sum_\nu h_\nu(t)\cdot\vec{H}_\nu(\vec{R}); \tag{65}$$

where $\vec{E}_\nu, \vec{H}_\nu$ are the homogeneous problem (Eq.(60)) solutions, $-\varphi$ is the Poisson Eq.(63) solution. The dimensionless $e_\nu(t), h_\nu(t)$ functions of time are defined under similar to sec.A1.1 consideration of the zero integral $\int\limits_{S_r}\left([\vec{E},\vec{H}_\nu], d\vec{S}\right)$ at the substitutions from Eq.(64,65) with the use of the orthogonality property:

$$\omega_\nu e_\nu(t) - \frac{dh_\nu(t)}{dt} = \frac{1}{W_\nu}\int\limits_V\left(\vec{H}_\nu, \vec{m}\right)dV, \tag{66}$$

[14] The inconsistency between the formal and real units of the fields from behind dimensionless W_ν value is not a problem at simulation, however $W_\nu = W$ form is preferable at analytical analysis.

the same integration for $[\vec{H}, \vec{E}_\nu]$ vector product yields

$$\omega_\nu h_\nu(t) + \frac{de_\nu(t)}{dt} = -\frac{1}{W_\nu} \int\limits_V \left(\vec{E}_\nu, \vec{j}\right) dV. \tag{67}$$

It is notable that from the Eq.(65) representation in Maxwell Eq.(64) it follows that electric and magnetic currents may be also expanded

$$\vec{j} = -\varepsilon \cdot \mathrm{grad} \frac{\partial \varphi}{\partial t} + \sum_\nu \left(\int\limits_V \left(\vec{E}_\nu, \vec{j}\right) dV \right) \frac{\varepsilon \vec{E}_\nu}{W_\nu}, \qquad \vec{m} = \sum_\nu \left(\int\limits_V \left(\vec{H}_\nu, \vec{m}\right) dV \right) \frac{\mu \vec{H}_\nu}{W_\nu}. \tag{68}$$

Gradient summand in Eq.(68) can be expanded in terms of the potential eigenfunctions; the charge density can be expanded in terms of these potentials and the similar formal representation is possible for magnetic current. The orthonormalized set completeness ensures convergence not only in V-volume residual meaning but in partial domains also.

A1.3 Wall losses

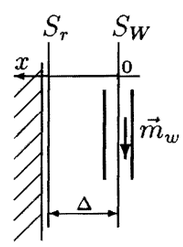

Tangential component of the real resonator electric field on the metallic surface can not be expressed directly by Eq.(65) since all the eigenfunctions electric field is normal to the surface. The problem is solved by introducing the additional magnetic current $\vec{m}_w$, which is distributed on S_W surface inside the volume at Δ distance from the S_τ surface. For the tangential component $\vec{E}_\tau$ at $x<0$ side of the surface with the zero component at $x \geq 0$ the continuity of the fields will be fulfilled at the superficial magnetic current $\vec{M}_w = \left[\vec{e}_x, \vec{E}_\tau\right]$, or $\vec{m}_w = \delta(x) \cdot \vec{M}_w$. The volumetric integral in Eq.(66) is transformed to the S_W surface one and realized condition of the zero component at $x \geq 0$ allows the passage to the limit:

$$\int\limits_V \left(\vec{H}_\nu, \vec{m}_w\right) dV = \int\limits_{S_W} \left([\vec{E}_\tau, \vec{H}_\nu], \vec{dS}\right) \overset{\Delta \to +0}{\longrightarrow} \int\limits_{S_\tau} \left([\vec{E}_\tau, \vec{H}_\nu], \vec{dS}\right). \tag{69}$$

The result is formally well known, however the model of ideal metal walls, which are covered by the magnetic current gives the means for correct consideration.

Inside the metal with σ conductivity the Maxwell equations are

$$\mathrm{rot}\vec{H}_M = \sigma \vec{E}_M, \qquad \mathrm{rot}\vec{E}_M = -\mu_0 \frac{\partial \vec{H}_M}{\partial t}. \tag{70}$$

In order for the mathematical treatment not to obscure physical aspects, the further analysis will be performed at Fourier transform $\mathbf{F}\{i\omega\}$; final conversion to real time should not present any problems. For any singled out small locality the metal surface can be considered as the plain and in local Cartesian system ($\vec{e}_x$ is directed into the metal, $y0z$ plain coincides with the surface) the $\vec{H}_M = \vec{e}_x \cdot H_{Mx} + \vec{e}_y \cdot H_{My} + \vec{e}_z \cdot H_{Mz}$ components solutions of Eq.(70) set are determined by the equations

$$\left(\frac{\partial^2 H_{Mu}}{\partial x^2} + \frac{\partial^2 H_{Mu}}{\partial y^2} + \frac{\partial^2 H_{Mu}}{\partial z^2} \right) = i\omega\mu_0\sigma \cdot H_{Mu}, \qquad u = x,\ y,\ z. \tag{71}$$

Only when $\frac{\partial^2 H_{Mu}}{\partial x^2} \gg \frac{\partial^2 H_{Mu}}{\partial y^2}, \frac{\partial^2 H_{Mu}}{\partial z^2}$ – for good conductor the characteristic distance at inward variation is defined by the skin-depth while the transverse variation distance is assumed to be commensurable at least with the wavelength – the equation takes the form

$$\frac{\partial^2 H_{Mu}}{\partial x^2} - i\omega\mu_0\sigma \cdot H_{Mu} = 0, \qquad u = x,\ y,\ z. \tag{72}$$

Outside the metal the cavity space magnetic field (Eq.(65)) has only $\vec{H}_{re}$ tangent component on the surface; consider the case when $\vec{H}_{re} = \vec{e}_y \cdot H_{re}$ (two-component consideration yields the same result). At the continuity $\vec{H}_{re} = \vec{H}_M|_{x=0}$ condition on the bound with the lack of unrestricted increase condition the Eq.(72) solution is

$$H_{My} = H_{re} \cdot e^{-x\sqrt{i\omega\mu_0\sigma}}, \qquad H_{Mx} = H_{Mz} = 0, \tag{73}$$

where the $\sqrt{i} = +(1+i)/\sqrt{2}$ value is accepted; according to Eq.(70) $\vec{E}_M = \frac{1}{\sigma} \cdot (\vec{e}_z \frac{\partial H_{My}}{\partial x} - \vec{e}_x \frac{\partial H_{My}}{\partial z})$. The similar to Eq.(71) approximation (for the first derivatives) and the tangential electric field continuity condition give

$$\vec{E}_{re} = \vec{E}_M|_{x=0} = -\vec{e}_z \sqrt{\frac{i\omega\mu_0}{\sigma}} \cdot H_{re}\ , \tag{74}$$

or in the general case $\vec{E}_{re} = \sqrt{\frac{i\omega\mu_0}{\sigma}} \cdot \left[\vec{H}_{re}, \vec{e}_x\right]$. It is well known absolutely correct result for a plain wave field since the neglected derivatives are merely zero in this case.

At the attempt to apply the last result for the cavity field (the commonly used method) the integral in Eq.(69) takes the form

$$\int_V \left(\vec{H}_\nu, \vec{m}_w\right) dV = \sqrt{\frac{i\omega\mu_0}{\sigma}} \cdot h_\nu A_{\nu\nu} + \sqrt{\frac{i\omega\mu_0}{\sigma}} \sum_{\substack{\xi \\ (\xi \neq \nu)}} h_\xi A_{\xi\nu}, \quad A_{\eta\zeta} = \int_{S_r} \left(\vec{H}_\eta, \vec{H}_\zeta\right) dS \tag{75}$$

(the modes are not orthogonal in the surface integral meaning, so $A_{\xi\nu} \neq 0$ in the general case); Eq.(66,67) set for h_ν, e_ν is

$$\begin{cases} e_\nu \omega_\nu \sqrt{\sigma} + h_\nu(-i\omega\sqrt{\sigma} - \frac{\sqrt{i\omega\mu_0} A_{\nu\nu}}{W_\nu}) = Y, \quad Y = \frac{\sqrt{i\omega\mu_0}}{W_\nu} \sum_{\substack{\xi \\ (\xi \neq \nu)}} h_\xi A_{\xi\nu} \\ e_\nu i\omega + h_\nu \omega_\nu = \Lambda_\nu, \quad \Lambda_\nu = -\frac{1}{W_\nu} \int_V \left(\vec{E}_\nu, \vec{j}\right) dV. \end{cases} \tag{76}$$

The set determinant $D = \sqrt{\sigma}(\omega_\nu^2 - \omega^2) - \frac{\omega\sqrt{\omega\mu_0} A_{\nu\nu}}{\sqrt{2} W_\nu} + i\frac{\omega\sqrt{\omega\mu_0} A_{\nu\nu}}{\sqrt{2} W_\nu}$ imaginary part is non-vanishing for any σ so the set solution is unique

$$\begin{cases} e_\nu = [(i\omega\sqrt{\sigma} + \frac{\sqrt{i\omega\mu_0} A_{\nu\nu}}{W_\nu})\Lambda_\nu + Y\omega_\nu] \cdot D^{-1}, \\ h_\nu = [\omega_\nu \sqrt{\sigma} \Lambda_\nu - i\omega Y] \cdot D^{-1}. \end{cases} \tag{77}$$

At $\sigma \to \infty$ (ideal metal) all the mode's fields can be in existence independently of one another. Examination of the Eq.(77) solution for $h_\nu = 0, e_\nu = 0$ case reveals that this is possible only at trivial $Y = 0, \Lambda_\nu = 0$ (all the modes are zero), because the homogeneous form of Eq.(77) for Y, Λ_ν has the same non-vanishing D determinant (the result is also verified by the direct passage $\sigma \to \infty$ for $\omega = \omega_\nu \neq \omega_\zeta$, $\Lambda_\nu = 0$, $\Lambda_\zeta \neq 0$ at definition of ζ-mode contribution to ν-mode field – the vanishingly small excitation yields finite contribution). Physically exact result for this case: $\Lambda_\nu = 0\ \forall h_\xi|_{\xi\neq\nu}$, $\forall \Lambda_\xi|_{\xi\neq\nu}$ can be obtained only under the $A_{\xi\nu} = 0\ \forall \xi \neq \nu$ correction. It is caused by inapplicability of the approximate boundary condition (Eq.(74)), generally observed in [14], as far as the summary field of arbitrary time-dependent modes with inhomogeneous spatial distributions can yield the arbitrary variation on the cavity surface (this can be clearly seen from the similar passage as σ increases at variable Λ_ζ excitation on $\omega \approx \omega_\zeta \neq \omega_\nu$ with Λ_ν excitation on $\omega \approx \omega_\nu$ – the field differs radically from the monochromatic plane wave). The correction insures right result for the single-mode case wherein the approximation is admissible. Generally, expression of the inegral in Eq.(69) can not contain any linear combinations of $h_\xi|_{\xi\neq\nu}$ [15] that is determined by the single-mode excitation and unexcitation conditions examination [16].

The physically correct result for the integral in Eq.(69) at the reverse transform to real time can be represented in the form

$$\frac{1}{W_\nu}\int\limits_V \left(\vec{H}_\nu, \vec{m}\right) dV = \frac{\omega_\nu}{Q_\nu}\cdot\left(h_\nu(t) + \frac{1}{\omega_\nu}\cdot\frac{dh_\nu(t)}{dt}\right) + \frac{\omega_\nu}{Q_\nu}\cdot\mathbf{F}^{-1}\left\{h_\nu(i\omega)\left(\sqrt{\frac{\omega}{\omega_\nu}} - 1\right)\cdot\left(1 - i\sqrt{\frac{\omega}{\omega_\nu}}\right)\right\}, \tag{78}$$

where

$$Q_\nu = \sqrt{2\omega_\nu\mu_0\sigma}\int\limits_V \mu\left(\vec{H}_\nu, \vec{H}_\nu\right) dV\cdot\left[\int\limits_{S_r} \mu_0\left(\vec{H}_\nu, \vec{H}_\nu\right) dS\right]^{-1}. \tag{79}$$

Second summand in Eq.(78) is obviously negligible; furthermore, the resonant properties provide even far less impact of the summand: analysis of the Eq.(66,67) set solution for $h_\nu(i\omega)$ reveals that for any excitation this term contribution (in relative energy sence) does not exceed $(1/Q_\nu)^2$ value (normalized squared modulus integration over $\omega \in (0, \infty)$) and the $(1/Q_\nu)^3$ value in the ν-mode bandwidth range.

Thus, Q_ν (Eq.(79)) is the quality factor of the resonator ν-mode, and the final form of

[15] Failure to take into account this property can lead to results [15], which can not be treated.

[16] It does not follow rigorously from Eq.(66,68) since the series are convergent in domains, but not in the surface integral meaning.

Eq.(66,67) set for $e_\nu(t), h_\nu(t)$ is

$$\begin{cases} (1+\frac{1}{Q_\nu})\frac{dh_\nu(t)}{dt} - \omega_\nu e_\nu(t) + \frac{\omega_\nu}{Q_\nu}h_\nu(t) = -\frac{1}{W_\nu}\int\limits_V \left(\vec{H}_\nu(\vec{R}), \vec{m}(\vec{R},t)\right) dV, \\ \frac{de_\nu(t)}{dt} + \omega_\nu h_\nu(t) = -\frac{1}{W_\nu}\int\limits_V \left(\vec{E}_\nu(\vec{R}), \vec{j}(\vec{R},t)\right) dV. \end{cases} \tag{80}$$

Appendix 2.

The prescribed under RF optimization (sec.2.5) value is in proportion to the even function integral $\int\limits_{-y_0}^{y_0} |F(\omega)|^2 d\omega$. Accordent to Eq.(32), the even $|D(\omega)|^2$ function expanding in powers of ω yields

$$\int\limits_0^{y_0} |D(\omega)|^2 |P(\omega)|^2 d\omega = |D(0)|^2 \int\limits_0^{y_0} |P(\omega)|^2 d\omega + \sum_{m=1}^{\infty} \frac{(|D(0)|^2)^{(2m)}}{(2m)!} \cdot (\omega_0)^{2m} A_m ,$$

where $A_m = \int\limits_0^{y_0} \left(\frac{\omega}{\omega_0}\right)^{2m} \frac{\sin^2\left(\frac{\pi\omega}{\omega_0}N\right)}{\sin^2\left(\frac{\pi\omega}{\omega_0}\right)} d\omega$ value for $y_0 < \frac{\omega_0}{2}$ allows evident estimations

$$A_m < \frac{1}{4}\int\limits_0^{y_0} \left(\frac{\omega}{\omega_0}\right)^{2m-2} \sin^2\left(\frac{\pi\omega}{\omega_0}N\right) d\omega < \frac{\omega_0}{4}\frac{1}{2m-1}\left(\frac{y_0}{\omega_0}\right)^{2m-1} ,$$

and the series converges to smaller than, e.g., $\frac{\omega_0}{8}\sum\limits_{m=1}^{\infty}\left|\frac{(|D(0)|^2)^{(2m)}}{(2m)!}\cdot(\omega_0)^{2m}\right|$ value, since $\{A_m\}$ is decreasing and $|D(\omega)|^2$ series is absolutely convergent, so the second term in the initial expression is limited with N increasing. However, the first term integral

$$\int\limits_0^{y_0} |P(\omega)|^2 d\omega = \frac{\omega_0}{\pi}\left(\chi\cdot\left(\sum_{k=1}^{N}\frac{\sin 2kg_0}{kg_0} - \frac{\sin 2\chi}{2\chi} + 1\right) - \frac{\cos g_0 \cdot \sin^2\chi}{\sin g_0}\right), \quad \chi = Ng_0, \ g_0 = \frac{y_0\pi}{\omega_0},$$

converges to $\frac{\omega_0}{2}N$ under the N increasing. Thus, with the use of $D(0) = \mathcal{E}_{out}$ value from Eq.(33), the result with any finite precision is

$$\int\limits_{-y_0}^{y_0} |F(\omega)|^2 d\omega = \mathcal{E}_{out}^2 N \cdot \frac{\omega_0\omega_r^2}{W_1^2} ,$$

since $N \gg 1$.

Appendix 3.

The optimization condition Eq.(23) for amplitude modulated signal with $\propto \cos(\omega_0 t + \varphi_0)$ carrier yields $\varphi_0 = \varphi$, since in accordance to Eq.(20) definition the phase characteristic $\alpha(\omega) = \varphi_0 + \breve{o}(\omega)$, where $\breve{o}(\omega)$ is some odd function. This φ_0 fixation (that is caused by the minimum minimorum searching) severely restricts further analysis and raises a question

as to whether there exists an optimum for $\varphi_0 \neq \varphi$ case. As far as the applied Cauchy-Schwarz inequality usually ensures the global extremum, the amplitude modulated signal optimum may be presupposed in this case also, and all other results in sec.2.5 do not stipulate $\varphi_0 = \varphi$ condition. However, for rigorous solution it is enough to consider $C_0(\omega) = C_{0e}(\omega) + C_{0o}(\omega)$ in the general form of the even $C_{0e}(\omega)$ and the odd $C_{0o}(\omega)$ parts sum and $\alpha(\omega) = \psi + \breve{o}(\omega) + \breve{e}(\omega)$ for any even $\breve{e}(\omega)$ (for definiteness $\breve{e}(0) = 0$), therewith Eq.(22) takes the form

$$\int_{-y_0}^{y_0}(x)\cdot(\overset{*}{x}+x\cos(2\varphi-2\psi-2\breve{e}(\omega)))d\omega = \frac{2\int_{-y_0}^{y_0}|F(\omega)|^2\,d\omega}{A^2} = \Lambda\,,\ \text{where}\, x = C_{0e}(\omega)+i\cdot C_{0o}(\omega)\,,$$

(*) – complex conjugate, and the inequality application leads to

$$\sqrt{\mathrm{E}_0\pi} \geq \frac{\Lambda}{\sqrt{2\Lambda - \int_{-y_0}^{y_0}|x|^2\sin^2(2\varphi-2\psi-2\breve{e}(\omega))d\omega}}\,.$$

The last form solution for $\mathrm{E}_0\pi$, where the influence of $\breve{e}(\omega)$ is limited for any phase characteristic, shows that the energy minimum corresponds to the equality case; this condition ($C_{0e}(0) \neq 0$, which follows from Eq.(19)) immediately gives $C_{0o}(\omega) = \breve{e}(\omega) = 0$ (the amplitude modulated signal only), therewith the equality case of the estimation is

$$\mathrm{E}_0\pi = \frac{\int_{-y_0}^{y_0}|F(\omega)|^2\,d\omega}{A^2\cos^2(\varphi-\psi)}\,.$$

Appendix 4.

Consider some function $g(\omega)$ that satisfies Eq.(36):

$$2g_{+2}(\omega+2\omega_0)e^{-i2\varphi} = (1+i\beta)g_0(\omega),$$

$\beta \in \Re = \mathrm{const}(\omega)$. The conditions use only (0) and ($+2\omega_0$) bands, and the Eq.(37) form function that coincides with $g_0(\omega)$ in (0) band can be constructed:

$$\mathbf{F}_0\left\{M(t)\cos(\omega_0 t+\varphi)\cos(\omega_0 t+\theta)\right\}(\omega) = M(\omega)\frac{\cos(\varphi-\theta)}{2} = g_0(\omega).$$

Therewith the ($+2\omega_0$) band spectrums also coincide, as far as their ratio

$$\frac{g_{+2}(\omega+2\omega_0)}{\mathbf{F}_{+2}\left\{M(t)\cos(\omega_0 t+\varphi)\cos(\omega_0 t+\theta)\right\}(\omega+2\omega_0)} = (1+i\beta)\cos(\varphi-\theta)e^{i(\varphi-\theta)}$$

comes out to 1 at the θ value that satisfies $\tan(\varphi-\theta) = -\beta$, so that Eq.(37) form presents all possible $g(\omega)$.

Appendix 5.

The spectrum width estimation by $\Omega^2 = \int\limits_{-\infty}^{\infty} |M_\Sigma(\omega)|^2 \omega^2 d\omega$ value, similarly to moment method [16,17], is of direct interest to the problem, because the spectrum contains the prescribed sharply defined $M_\Sigma(0)$ component, and $M_\Sigma(\omega)$ energy in $[-y_0, +y_0]$ band is prescribed also. The even $2\tau_v$ duration time-function $G(t)$, which is formed by symmetrically disposed time-varying parts of $f(t)$,
$G(\omega) = \mathbf{F}\left\{[\mathbf{1}(t+\tau_v) - \mathbf{1}(t-\tau_v)]\Big(f(\tau_v - t) + f(\tau_v + t)\Big) - f_s\right\}$, $\tau_v = (K-1)T + \zeta$, has the same Ω for any $f(t)$ that satisfies Eq.(43,42). To minimize the width, consider Cauchy-Schwarz inequality

$$\left(\int\limits_{-\infty}^{\infty} t^2 G(t)^2 dt\right)^{\frac{1}{2}} \left(\frac{\Omega^2}{2\pi}\right)^{\frac{1}{2}} \geq \left|\int\limits_{-\infty}^{\infty} tG(t)\frac{dG(t)}{dt}dt\right| = \frac{1}{2}\int\limits_{-\infty}^{\infty} G(t)^2 dt\,,$$

where additional condition $(f^2)'(0) = 0$ is used, so that

$$\Omega \geq \sqrt{\frac{\pi}{2}}\left(2\int\limits_{0}^{\tau_v} f(t)^2 dt\right)^{\frac{1}{2}} \frac{1}{T_G}\,,$$

where $T_G = \left(\int\limits_{-\tau_v}^{\tau_v} t^2 G(t)^2 dt\right)^{\frac{1}{2}} \left(\int\limits_{-\tau_v}^{\tau_v} G(t)^2 dt\right)^{-\frac{1}{2}}$ – equivalent duration of $G(t)$. The integral in the last estimation is limited, since it presents the energy of the beam excitation in $t \in [0, \tau_v]$ interval [17], $T_G \leq \tau_v$ as well, and Ω minimum is achieved in the equality case. As far as the equality condition $\frac{dG(t)}{dt} \propto tG(t)$ is satisfied at $\tau_v \to \infty$ for Gauss time-dependence $G_\infty(t)$ only, the real function (Eq.(42)) can not contain $G_\infty(t)$ form exactly; however, under the use of the closely corresponding form (Eq.(46)) the loss

$$\frac{\Omega}{\Omega_{min}} = \frac{\sqrt{\mathrm{erf}(\sqrt{2}\frac{u}{a}) - \frac{1}{\sqrt{2\pi}}\frac{u}{a}e^{-2(\frac{u}{a})^2}}}{1 - e^{-(\frac{u}{a})^2}}\,, \quad \mathrm{erf} - \text{error function}\,,$$

is not very substantial for $u/a > 2$, Fig. 7.

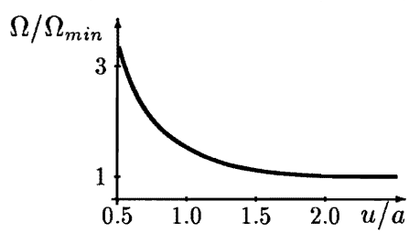

Fig. 7. Loss in the spectrum width value.

[17] To be more precise, the energy of this signal in $[-y_0, +y_0]$ band is prescribed, but it can not be determined under $N \gg K$ condition, see Eq.(47).

Appendix 6.

Under conventional power parameters application the definition of the resonator unloaded quality factor yields (W_1 is the doubled stored energy at resonance)

$$P_l = \frac{A^2 W_1 \omega_r}{2Q_r},$$

where P_l – power losses in the cavity; $P_b = \omega_0 \mathcal{E}_{out}/2\pi$ is the beam power and the ratio $b = P_b/P_l$ will present the main characteristics. Since the beam excitation signal is defined by Eq.(39) with $M(0)$ value from Eq.(40), the ω_0 spectrum is

$$V(\omega_0) = \frac{\omega_r N \mathcal{E}_{out}}{A W_1 \cos(\varphi - \theta)} e^{i(\theta \pm \pi)};$$

Eq.(16) indicates the sign $\frac{V_0}{A\omega_r}\cos(v_0 - \varphi) \leq 0$, and assuming for definiteness $A > 0$ the Eq.(29) give

$$\frac{V_0}{A\omega_r}\cos(v_0 - \varphi) = -b \cdot \frac{\omega_r}{Q_r}; \quad \cos(\varphi - \theta) \geq 0.$$

Now the use of Eq.(16) and (5) yields the loaded quality factor of the matched resonator

$$Q_L = \frac{Q_r}{2 + b},$$

the equivalent unloaded quality factor (Eq.(17)) is

$$Q_{eq} = Q_r \cdot \frac{\omega_r}{\omega_0} \cdot \frac{1}{1 + b},$$

and the generalized deviation (Eq.(15)) is

$$\xi_0 = Q_r \cdot \frac{\omega_0^2 - \omega_r^2}{\omega_0 \omega_r} = b \cdot \tan(\varphi - \theta).$$